THE ASTROPHYSICAL JOURNAL, 339:742–751, 1989 April 15

KINEMATIC EVIDENCE FOR A RELATIVISTIC KEPLERIAN DISK: ARP 102B

KAIYOU CHEN AND JULES P. HALPERN[1]
Columbia Astrophysics Laboratory, Columbia University

AND

ALEXEI V. FILIPPENKO[2]
Astronomy Department, University of California, Berkeley
Received 1988 April 18; accepted 1988 September 16

ABSTRACT

The broad emission lines of the elliptical galaxy Arp 102B have peaks which are significantly displaced in velocity with respect to the host galaxy of the active galactic nucleus (AGN). We calculated line profiles for a Keplerian disk, including relativistic effects which were not treated rigorously in previous papers. We found an excellent fit of the resulting double peaked, asymmetric profiles to the Hα line of Arp 102B, yielding an accurate determination of several parameters of the disk. The inner and outer radii are ~ 250 and ~ 1000 in units of GM/c^2. The inclination angle is $33^\circ.5 \pm 5^\circ.5$. The Hα emissivity peaks at a radius of $\sim 450GM/c^2$. Both the models and the data show that relativistic effects of Doppler boosting and gravitational and transverse redshift cause observable asymmetries when the velocity is of order $0.02c$, typical of the broad-line velocities in AGNs. We conclude that the line profile of Arp 102B shows the most convincing direct kinematic evidence for rotation in any AGN. The gravitational energy available in a standard accretion disk is marginally sufficient to power the line emission locally, so an extra source of heating, possibly photoionization by radiation from the inner disk or central nonthermal continuum, may be required. We speculate that ion-supported tori might account for the unusual properties of Arp 102B and other broad-line radio galaxies, including a far-infrared peak at 25 μm.

Subject headings: galaxies: individual (Arp 102B) — galaxies: internal motions — galaxies: nuclei — galaxies: Seyfert — line profiles

I. INTRODUCTION

The theory that rotating accretion disks are responsible for the broad emission-line profiles in quasars is a recurrent idea which has met with limited observational support. Despite the ubiquity of angular momentum in astrophysical systems, the evidence for rotation in quasars is at best indirect (see Filippenko 1988 for a recent review). The fit of accretion disk models to the broad-band *continuum* spectrum of AGNs (Shields 1978; Malkan and Sargent 1982; Sun and Malkan 1988; Czerny and Elvis 1987) provides circumstantial evidence for rotation, as do the alignment of radio jets, which require a stable axis (see, e.g., Begelman, Blandford, and Rees 1984). The obstacle to fitting disk-like *emission lines* is that the predicted asymmetries and double-peaked profiles generally do not match the observations of quasars (Mathews 1982, and references therein), which favor radial inflow or outflow of clouds. On the positive side, van Groningen (1983) showed that the wings of the lines in several Seyfert galaxies agree with Keplerian rotation. Photoionization of clouds having a small volume filling factor (e.g., Kwan and Krolik 1981) is generally accepted as the line emission mechanism, although Collin-Souffrin *et al.* (1980) and Collin-Souffrin (1987) have argued that high-density material in an accretion disk may be required to account for the strong Fe II lines which are sometimes seen.

There are in fact a small number of AGNs which show double-peaked broad-line profiles. Many of these are radio galaxies such as 3C 390.3 and 3C 382 (Osterbrock, Koski, and Phillips 1976). It has been suggested that the emission lines in 3C 390.3 come from a disk (Oke 1987; Perez *et al.* 1988). Alternatively, Gaskell (1988) interprets the double peaks as evidence for two separate broad-line regions, hence a binary black hole.[3] Probably the most distinctive example of this phenomenon is the unusual elliptical AGN Arp 102B ($z = 0.02438$), which is also a low-luminosity broad-line radio galaxy (Stauffer, Schild, and Keel 1983; Puschell *et al.* 1986; Halpern and Filippenko 1988). Because of the large velocity of the displaced peaks, ~ 5000 km s^{-1}, the spectroscopic monitoring by Halpern and Filippenko (1988) ruled out the binary black hole hypothesis unless the sum of the masses of the black holes is $2 \times 10^9\ M_\odot$ or greater, an unlikely circumstance given the low luminosity of Arp 102B.

The line profile of Arp 102B is perhaps the best direct kinematic evidence for rotation in an AGN. In § II, we rederive the theoretical line profile of a Keplerian disk, including relativistic effects which were not treated correctly in previous attempts (Mathews 1982 and references therein). In § III, we demonstrate a good fit of the model line profile to Arp 102B, in which relativistic effects are apparent. As a result, several parameters

[1] Guest Observer, *International Ultraviolet Explorer* Satellite.

[2] Guest Observer, Palomar Observatory, which is owned and operated by the California Institute of Technology. Observations also made at Lick Observatory, which is owned and operated by the University of California.

[3] Note that this point of view has some severe difficulties if we assume that all of the line broadening is due to Keplerian motions. As Penston (1988) succinctly stated, "The line profile from a binary black hole system is not the sum of the profiles of the two holes." This is because low-velocity gas effectively orbits the center of mass of the binary system, producing a *single* core. High-velocity gas, on the other hand, is close to each of the black holes and gives rise to double peaks in the *wings* of the line. The separation between the two peaks in a broad wing is comparable to the relative orbital speed of the system, so they essentially merge together. Thus, widely spaced peaks are *not* the signature of broad-line regions gravitationally bound to a binary black hole.

of the Hα-emitting region are determined, including the inclination angle. Some additional line and continuum data are presented in § IV, which discusses Arp 102B in the context of other low-luminosity AGNs.

II. LINE PROFILE OF A KEPLERIAN DISK

We assume for the calculation a geometrically thin, Keplerian disk with inner and outer radii r_1 and r_2, respectively, rotating about a black hole of mass M. The geometry is shown in Figure 1. We use the usual spherical polar coordinate system (r, θ, φ) with the observer on the positive z-axis at $z = \infty$. The rotation axis z' of the disk is inclined by an angle i in the x, z plane. Azimuthal angles φ and φ' are measured with respect to the x and x' axes, respectively. The disk rotates in the direction of increasing φ' (Fig. 1). The relation between the angles is

$$\sin \varphi' = \sin \theta \sin \varphi , \tag{1}$$

$$\cos \theta = \sin i \cos \varphi' . \tag{2}$$

It is straightforward to transform directly from the rest frame of the emitting particle to the observer's frame. The Schwarzschild metric is assumed. To calculate the observed frequency of a photon, we first note that the four-momentum, p^α, of a photon originating at radius r is (Misner, Thorne, and Wheeler 1973)

$$p^\alpha = h\nu\{(1 - 2M/r)^{-1}, - [1 - b^2(1 - 2M/r)r^{-2}]^{1/2}, -br^{-2}, 0\} \tag{3}$$

where $h\nu$ is the observed energy of the photon and b is the impact parameter at infinity. We set $c = G = 1$ throughout this paper. The four-velocity, u_α, of an emitting particle in the Keplerian disk at r is

$$u_\alpha = \gamma\left\{\left(1 - \frac{2M}{r}\right)^{1/2}, 0, \frac{-M^{1/2}r^{1/2}}{(1 - 2M/r)^{1/2}} \sin i \sin \varphi, \frac{M^{1/2}r^{1/2} \sin \theta}{(1 - 2M/r)^{1/2}} (1 - \sin^2 i \sin^2 \varphi)^{1/2}\right\}, \tag{4}$$

where γ is $(1 - v^2)^{-1/2} = [1 - M/(r - 2M)]^{-1/2}$. It follows that $h\nu_e$, the energy of the photon as measured in the rest frame of the emitting particle, is

$$h\nu_e = p^\alpha u_\alpha = h\nu\left(1 - \frac{3M}{r}\right)^{-1/2}\left(1 + \frac{bM^{1/2}}{r^{3/2}} \sin i \sin \varphi\right) . \tag{5}$$

This result was also derived by Luminet (1979).

The total *observed* line flux F is the integral of the specific intensity I_ν over frequency and over the solid angle $d\Omega$ subtended in the observer's sky by the luminous disk,

$$F = \iiint I_\nu \, d\nu \, d\Omega . \tag{6}$$

Due to light bending, the solid angle in the emitting frame is not the same as the solid angle in the observer's frame. It is convenient to express the solid angle in the observer's sky in terms of the impact parameter b as

$$d\Omega = \frac{b \, db \, d\varphi}{d^2} , \tag{7}$$

where d is the distance to the AGN. It is also necessary to express the specific intensity of a line in the emitting frame by a δ-function at the rest frequency ν_0 of emission:

$$I_{\nu_e} = \epsilon(\xi)\delta(\nu_e - \nu_0) \text{ ergs cm}^{-2} \text{ s}^{-1} \text{ Hz}^{-1} \text{ sr}^{-1} . \tag{8}$$

For convenience, here $\xi = r/M$ is the dimensionless radius, and $\epsilon(\xi)$ is the surface emissivity which is assumed to vary with radius as a power law with index q,

$$\epsilon(\xi) = \frac{\epsilon_0}{4\pi} \xi^{-q} \text{ ergs cm}^{-2} \text{ s}^{-1} \text{ sr}^{-1} . \tag{9}$$

Combining equations (6) and (8), and remembering that $I_\nu/\nu^3 = I_{\nu_e}/\nu_e^3$, a Lorentz invariant, the total observed flux in the line is

$$F = \iint \epsilon(\xi)(\nu/\nu_0)^4 \, d\Omega . \tag{10}$$

Now we introduce the quantities X and F_X such that $1 + X = \nu/\nu_0$ and $F = \int F_X \, dX$. From equations (7) and (10),

$$F_X = \frac{1}{d^2} \int \epsilon(\xi)(1 + X)^4 b \, db \, \frac{d\varphi}{dX} . \tag{11}$$

Up to this point, the equations are derived correctly in the Schwarzschild metric without any approximation. In the weak-field approximation, to first order in M/r, the impact parameter b can be written as (Adler, Bazin, and Schiffer 1975)

$$b \approx r \sin \theta + \frac{M}{2 \sin \theta} (3 - 4 \cos \theta + \cos 2\theta) . \tag{12}$$

This expression is valid when the second term is much smaller than the first term, which is true for the disk parameters of interest here. Combining equations (5) and (12) with the help of equations (1) and (2), we have that

$$1 + X = (1 - 3/\xi)^{1/2}(1 + \xi^{-1/2} \sin i \sin \varphi')^{-1} , \tag{13}$$

Note that photons emitted at φ' and $\pi - \varphi'$ have the same X in the weak field approximation. Using equations (1), (2), (9), and (12), equation (11) becomes

$$F_X = \frac{2\epsilon_0 M^2 \cos i}{4\pi d^2} \int_{\xi_a}^{\xi_b} d\xi \, \frac{\alpha(1 + X)^3 \xi^{3/2 - q}}{[(1 + X)^2 \sin^2 i - \beta]^{1/2}} \times \left\{1 + \xi^{-1}\left[\frac{2(1 + X)^2}{(1 + X)^2 \cos^2 i + \beta} - 1\right]\right\} . \tag{14}$$

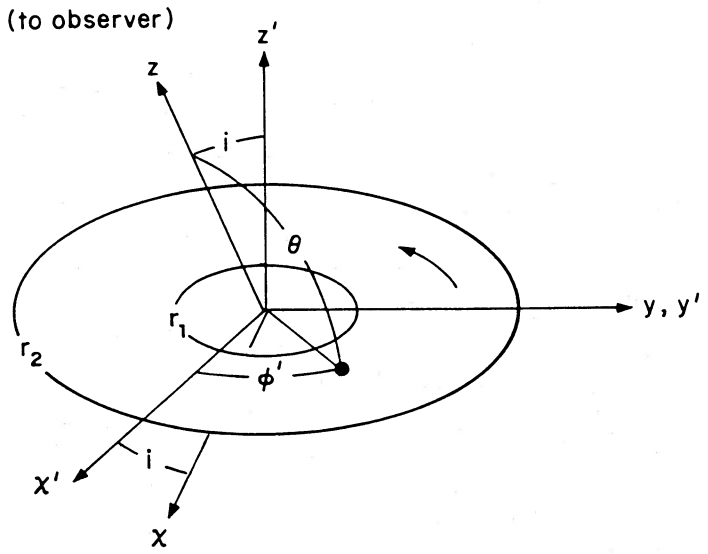

FIG. 1.—Geometry used in this paper

Here we have defined $\alpha = (1 - 3/\xi)^{1/2}$ and $\beta = \xi(1 + X - \alpha)^2$. The limits of integration are $\xi_a = \max(\xi_1, \xi_{c1})$ and $\xi_b = \min(\xi_2, \xi_{c2})$. The ξ_{c1} and ξ_{c2} are roots of equation (13) when $\sin \varphi' = -1$ and 1, respectively, for a given X. Equation (14) represents the dimensionless line profile of an optically thick disk since the emissivity is assumed independent of angle relative to the normal of the disk. The second term in brackets, of order ξ^{-1}, is due to the light bending.

To compare directly with an observed spectrum, f_ν, in flux units, one would replace M^2 in equation (14) by $(GM/c^2)^2$, and note that $F_X\, dX = f_\nu\, d\nu$. Therefore

$$f_\nu = \frac{G^2}{\nu_0 c^4} F_X \text{ ergs cm}^{-2} \text{ s}^{-1} \text{ Hz}^{-1} . \quad (15)$$

When fitting to an observed line, the parameters ξ_1, ξ_2, i, and q can, in principle, all be determined by the shape of the line, while the normalization fixes the product $\epsilon_0 M^2$. Since the model involves only the dimensionless radius $\xi = r/M$, one cannot determine the mass or the absolute emissivity from the line profile alone.

In the case of an optically thin disk, the emissivity of equation (9) will be increased by the factor $1/\mu$, where μ is the cosine of the angle between the emitted photon and the normal to the disk. The four-velocity of a photon emerging normal to the disk is

$$n_\alpha = \left\{1, 0, \frac{r(1 - \sin^2 i \sin^2 \varphi)^{1/2}}{(1 - 2M/r)^{1/2}}, \frac{r \sin\theta \sin i \sin\varphi}{(1 - 2M/r)^{1/2}}\right\}, \quad (16)$$

and $p^\alpha n_\alpha = p^0 n_0(1 - \mu)$. Therefore, we find

$$\mu = (b/r)(1 - 2M/r)^{1/2}(1 - \sin^2 i \sin^2 \varphi)^{1/2} . \quad (17)$$

By using equations (1), (2), and (12), equation (17) can be rewritten as

$$\mu = \left(1 - \frac{2}{\xi}\right)^{1/2}\left(1 + \frac{3 - 4\cos\theta + \cos 2\theta}{2\xi \sin^2\theta}\right)\cos i . \quad (18)$$

Note that $\mu \to \cos i$ as $\xi \to \infty$. When the factor $1/\mu$ is included in the emissivity, the line profile for the optically thin disk in the weak-field limit is

$$F_X = \frac{2\epsilon_0 M^2}{4\pi d^2}\int_{\xi_a}^{\xi_b} d\xi \frac{\alpha(1 - 2/\xi)^{-1/2}(1 + X)^3 \xi^{3/2 - q}}{[(1 + X)^2 \sin^2 i - \beta]^{1/2}} . \quad (19)$$

Equation (14), the thick disk case, can be most directly compared with the results of Mathews (1982). The first term in the integral has the factor $(1 + X)^3$ in the numerator, whereas Mathews' equation (3) has $(1 + X)^2$. This is because Mathews' equation (1) did not correctly treat the specific intensity as a δ-function *in the emitting frame*, as we did in equation (8). Each factor of $1 + X$ is significant; for example, it results in an extra difference of $\sim 4\%$ in the relative heights of the red and blue peaks for $v \approx 0.02c$. There is also an error in Mathews' transformation of the emissivity immediately following his equation (1). The expression in his second brace should be equal to $(1 - 2/\xi)^{3/2}$ rather than $(1 - 2/\xi)^{-1/2}$, since the gravitational redshift should decrease the observed energy. This can be verified because the entire transformation must leave I_ν/ν^3 invariant. If these two corrections are applied to Mathews' equation (3), then it would agree with the first term in our equation (14). Our second term, of order ξ^{-1} smaller than the first, comes from the inclusion of light bending to first order in M/r. Finally, Mathews does not include the factor $\cos i$ appropriate to the optically thick case.

Gerbal and Pelat (1981) calculated just the emission from a thin ring. We can compare the first part in the integrand of our equation (14) with their equation (6). Gerbal and Pelat have the correct power of $1 + X$ in the numerator. Their only error is that their quantity β, corresponding to our $\sin i/\xi$, should be squared. This may be an algebraic error: the assumptions leading up to it are correct. Gerbal and Pelat (1981) also neglected light bending, but this is not consistent since it gives a correction of order M/r, which is the same order kept in their calculation.

Finally, we note that since equations (14) and (19) were derived under the weak field approximation, they are independent of the metric chosen. The Kerr metric will yield the same result as long as equation (12) is valid. Thus, the observations of optical emission lines cannot, in general, reveal any information about the rotation of black hole since $\xi \gg 1$. Perhaps X-ray emission lines, which could come from a region closer to the black hole, will be discovered in the future, permitting tests of the Kerr models as assumed by Sun and Malkan (1988) in their continuum modeling.

III. EVIDENCE FOR A KEPLERIAN DISK IN ARP 102B

a) *Model Fits*

We used equation (14) to fit the observed broad Hα line profile of Arp 102B. The data were taken from Halpern and Filippenko (1988). There were small changes in the line profile over the 5 yr of observation, so we decided to average all the spectra taken between 1985 and 1987 before fitting. The continuum was approximated by a straight line between 6200 and 7100 Å and subtracted. Since the continuum is mostly starlight, we also investigated subtractions using the spectrum of NGC 4339 as a template (see Filippenko and Sargent 1988), a method which yields virtually the same line profile.

Figure 2 shows a range of fits which can reasonably be accommodated by the broad Hα profile. The disk models do not account for all of the Hα flux, especially near zero velocity; therefore, we have taken the approach that the disk-like component should be fitted by eye to as much of the flux as possible without exceeding the observation at any point. Two features of the data very much support the disk model. First, the blue peak is higher than the red peak, which is consistent with Doppler boosting. Second, there is a net redshift of the high-velocity portions of the profile due to gravitational redshift. Unfortunately, the strength of the narrow forbidden lines makes it difficult to fit the broad wings of the Hα line or its red peak. In particular, the limiting factor in the accuracy of the fit is the uncertainty in the amount of flux to attribute to the [S II] lines. The best fit (*heavy line*) corresponds to the parameters $i = 33\overset{\circ}{.}5$, $\xi_1 = 400$, $\xi_2 = 1000$, and $q = 3.1$. Models a and b determine the range of uncertainty in the parameters. Model a corresponds to $i = 28°$, $\xi_1 = 270$, $\xi_2 = 720$, and $q = 3.2$, whereas model b corresponds to $i = 39°$, $\xi_1 = 550$, $\xi_2 = 1400$, and $q = 3.0$. The inclination angle i can be determined fairly accurately as $i = 33\overset{\circ}{.}5 \pm 5\overset{\circ}{.}5$, because the effects of gravitational and transverse Doppler shift break the degeneracy with respect to inclination angle and radius in Keplerian motion. The emissivity index q is determined by the steepness of the blue side of the profile, and can be conservatively estimated as 3.1 ± 0.3.

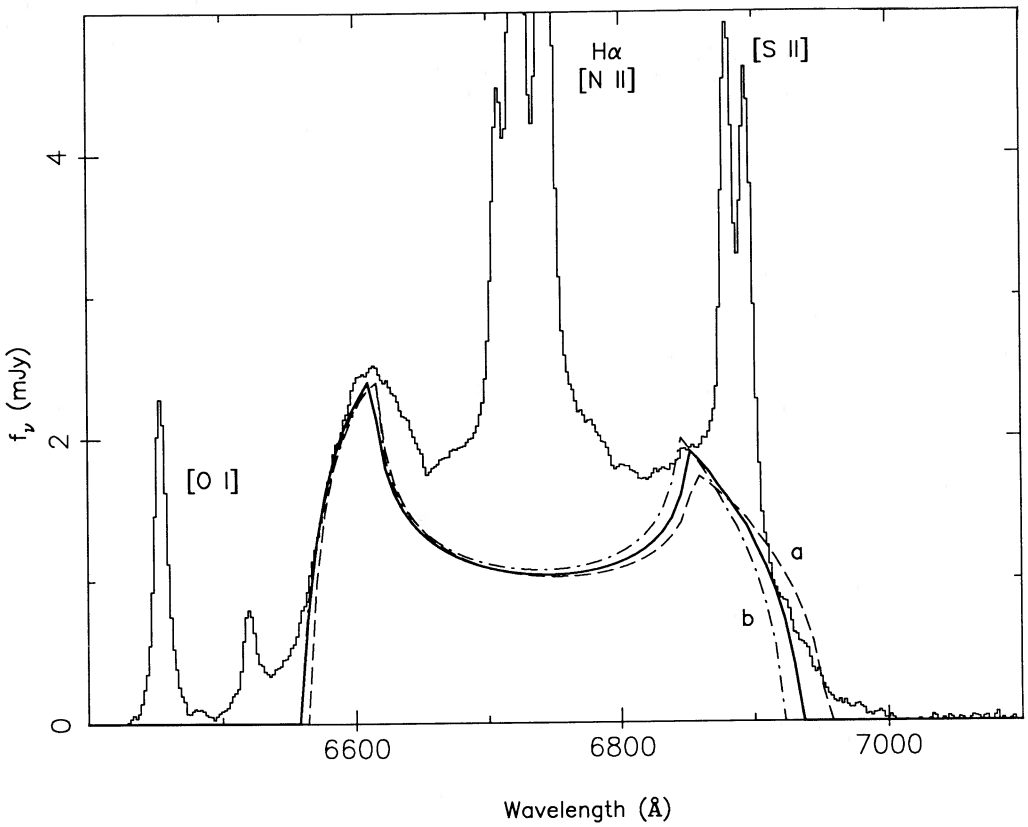

FIG. 2.—The disk model fits to the Hα line profile of Arp 102B. The best fit (*heavy line*) corresponds to $i = 33°.5$, $\xi_1 = 400$, $\xi_2 = 1000$, and $q = 3.1$. Line (a) (*dashed line*) corresponds to $i = 28°$, $\xi_1 = 270$, $\xi_2 = 720$, and $q = 3.2$. Line (b) (*dot-dashed line*) corresponds to $i = 39°$, $\xi_1 = 550$, $\xi_2 = 1400$, and $q = 3.0$. Observed wavelength is plotted.

The addition of another component to the inner part of the disk greatly improves the fit to the wings of the line. If, instead of having a sharp inner boundary, we allow the emissivity to first increase with radius and then decrease, a much better fit to the data is achieved with $i = 33°.5$, $q = 3.0$ for $450 < \xi < 1020$ and $q = -3.0$ for $250 < \xi < 450$. This model, illustrated in Figure 3, is more appealing since the emissivity does not have a large discontinuity at the inner edge. Of course, the derived parameters apply only to the Hα-emitting region of a disk which probably extends to larger as well as smaller radii. The peak Hα flux from the disk is 5×10^9 ergs cm^{-2} s^{-1} at $\xi = 450$, for an assumed mass of $10^8\ M_\odot$. Figure 4 shows the residual spectrum after subtraction of the model from the original spectrum of the galaxy. The remaining line profile has broad Hα wings similar to those in a Seyfert 1.5 galaxy. Obviously, the disk model does not account for all the broad-line emission. The most troublesome feature is the small bump at ~6630 Å, which is left because the blue peak is significantly broader than the cusp-like model profile. We do not present any further fine tuning of the model here, although there are at least three realistic effects which can improve the fit, and allow the disk model to account for a larger fraction of the line. First, the inclusion of local broadening due to turbulence or electron scattering would broaden the peaks and reduce their heights relative to the low-velocity portion of the line. Second, the use of an emissivity law with a continuously variable slope would have a similar effect. Third, any optical depth in the line will also reduce the heights of the peaks (Horne and Marsh 1986). Fits incorporating the first two effects will appear in Halpern and Chen (1989).

b) *Physical Interpretation*

One may interpret these results in terms of the standard geometrically thin accretion disk model (Shakura and Sunyaev 1973). Radiation of the disk's gravitational energy requires that the total flux from the top and bottom surfaces as a function of radius is

$$2F(\xi) = 1 \times 10^{12} M_8^{-2} \dot{M}_{24}\, \xi_{100}^{-3} [1 - (6/\xi)^{1/2}] \text{ ergs cm}^{-2}\text{ s}^{-1}\ , \quad (20)$$

where M_8 is the black hole mass in units of $10^8\ M_\odot$, $\dot{M}_{24}$ is the accretion rate in units of 10^{24} g s^{-1}, and ξ_{100} is $(\xi/100)$. The estimated accretion rate is that which will produce the observed soft X-ray luminosity of 9×10^{42} ergs s^{-1} at an efficiency of 1%, and the estimated mass is appropriate for Seyfert galaxies having the observed X-ray luminosity (Wandel and Mushotzsky 1986). The theoretical flux at $\xi = 450$ is 1×10^{10} ergs cm^{-2} s^{-1}, which is roughly equal to the fitted Hα flux of 5×10^9 ergs cm^{-2} s^{-1} at this radius. This conclusion is independent of the black hole mass, since both the measured ϵ_0 and the theoretical flux $F(\xi)$ vary as M^{-2}. Therefore, a local excitation process for the lines is possible only if virtually all the available energy is converted to line emission. More likely, heating of a disk chromosphere by radiation from the inner disk or central nonthermal source is needed to power the line

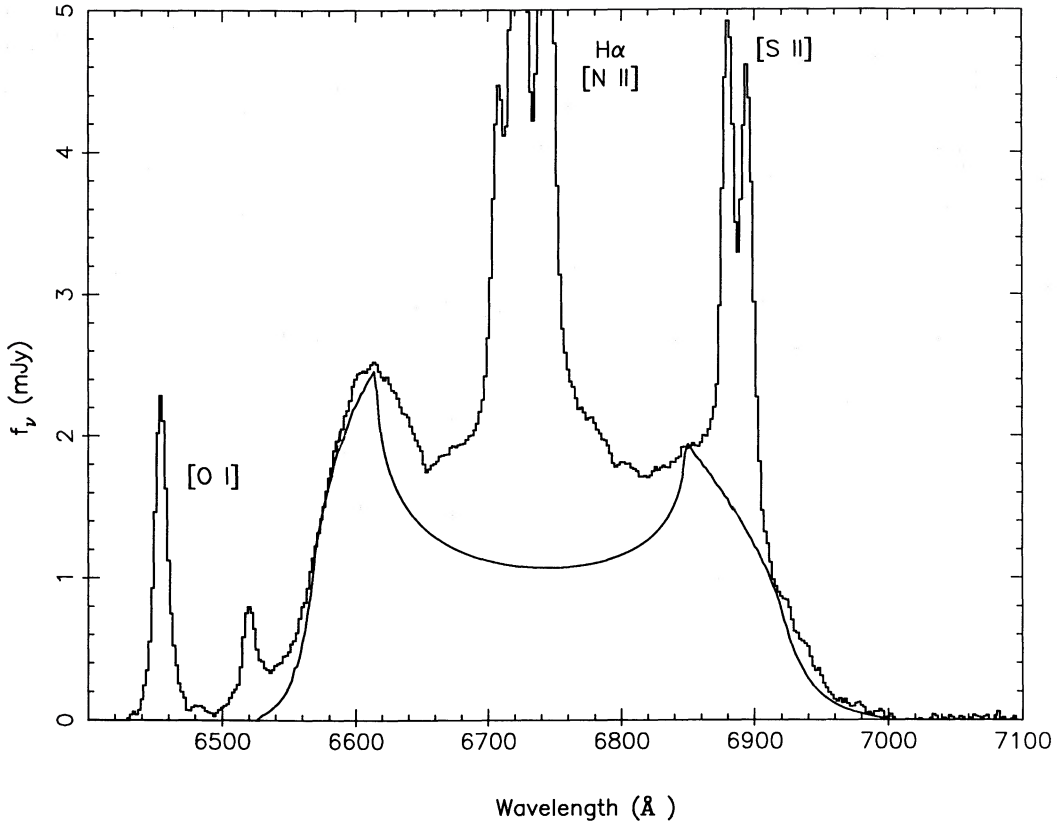

FIG. 3.—The parameters of the fit are $i = 33°.5$, $q = 3.0$ for $450 < \xi < 1020$, and $q = -3.0$ for $250 < \xi < 450$. Observed wavelength is plotted.

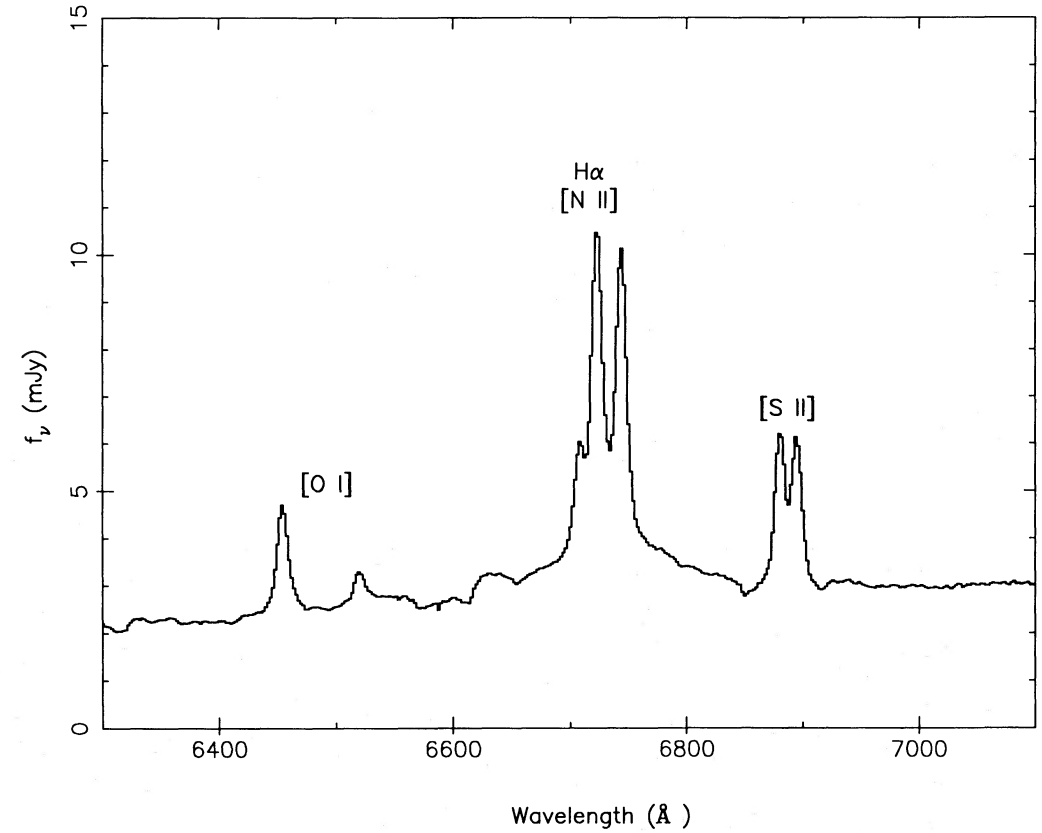

FIG. 4.—The residual spectrum of Arp 102B after subtraction of the model disk emission-line component. Observed wavelength is plotted.

TABLE 1

NEW OBSERVATIONAL DATA: ARP 102B

Wavelength	Flux[a]
100 μm	<720[b] (mJy)
60 μm	290
25 μm	280
12 μm	<140[b]
3000 Å	0.3
1500 Å	<0.08
Lyα	2.8×10^{-13} ergs cm^{-2} s^{-1}
Hα	b: 5.46×10^{-13}
	n: 0.49×10^{-13}
Hβ	b: 8.28×10^{-14}
	n: 1.15×10^{-14}
Hγ	b: 2.56×10^{-14}
	n: 0.47×10^{-14}

[a] Broad and narrow components are indicated by b and n, respectively.

[b] 5 σ upper limit.

emission. This requirement was also deduced by Collin-Souffrin (1987) for the line emission from AGN disks in general.

If the disk is optically thick, then the effective blackbody temperature as a function of radius is

$$T_{\rm eff}(\xi) = 9.7 \times 10^3 M_8^{-1/2} \dot{M}_{24}^{1/4} \xi_{100}^{-3/4} [1 - (6/\xi)^{1/2}]^{1/4} \text{ K}, \quad (21)$$

The effective temperature is apparently less than 5000 K in the region of observed line emission. Williams (1980) and Tylenda (1981) have shown that Balmer line emission is possible from accretion disks in cataclysmic binaries when the temperature is 7000 K or less. However, the resulting Balmer decrements are very flat, with Hβ ≃ Hα, not at all like the ratio Hα/Hβ ≈ 6.6 observed in Arp 102B (see Table 1). More likely, the disk is not optically thick, so that the actual electron temperature will be higher, producing recombination Balmer line ratios like those observed. In addition, any photoionization would raise the temperature and the line emissivity. This photoionizing flux could come directly from the inner parts of the disk, or could be scattered down from a highly ionized corona above the disk.

The fit to the emissivity index, $q = 3.1 \pm 0.3$, could possibly be used to discriminate between emission mechanisms for the lines. For example, equation (20) shows that the disk emissivity varies as r^{-3}, just like the emission-line emissivity in the "outer" part of the fit. It is tempting, therefore, to associate the line emission with some fixed efficiency of local conversion of disk gravitational energy to line luminosity, except that we have already estimated that this energy may not be enough. However, $q = 3$ would also result from an isotropic source of illumination concentric with a thin disk providing that the source is significantly smaller than the disk (Mardaljevic, Raine, and Walsh 1988). Clearly, the composite nature of the line profile, as well as the small range of radius (roughly a factor of 4) over which emission occurs, makes it difficult to interpret q physically. Another important question is what sets the inner and outer boundaries of the emission region. Perhaps these radii are the points where the temperature becomes too hot and too cold, respectively, to emit Balmer lines. Once again, equation (21) does not offer a logical solution in terms of blackbody emission, since the effective temperature is generally lower than one would expect for recombination Balmer emission. The properties of an overlying chromosphere may be the more relevant quantities.

For inner and outer radii of 250 and $1000GM/c^2$, the rotation periods are $\sim 0.4 M_8$ and $3 M_8$ yr, respectively. Therefore, we should expect to see changes in the line profile on a time scale of a year if the disk is not perfectly uniform. In fact, there have been slight variations from year to year (see Fig. 1 of Halpern and Filippenko 1988). If the mass is $10^8\ M_\odot$ or less, it may be possible to watch inhomogeneities propagate around the disk in a few years, and thus to measure the mass of the black hole. Similarly, light travel times are of order 10^5 s, so that short-term variations on a time scale of days are possible if the line emission is due to heating by a central, variable X-ray source. Thus, simultaneous continuum and line profile observations could in principle provide an independent confirmation of the rotating disk theory via the reverberation mapping technique (Blandford and McKee 1982), and also provide a measurement of M.

IV. ARP 102B: ADDITIONAL OBSERVATIONAL DATA

A spectrum of Arp 102B covering the range 3760–5480 Å was obtained with the Hale 5 m reflector at Palomar Observatory on 1988 February 8 UT. Subtraction of a weak nonstellar continuum ($f_\nu \propto \nu^{-1}$) and the appropriately adjusted template galaxy IC 4889 (Filippenko and Halpern 1984) produced the net emission-line spectrum shown in Figure 5. Broad Hβ emission is present, and has virtually the same shape as the corresponding Hα profile (Fig. 6). Unfortunately, the strong [O III] λλ4959, 5007 lines contaminate the red wing of the broad emission, as was the case with the [S II] λλ6716, 6731 doublet near Hα. The broad Hγ line is also visible in Figure 5. Although noisy, the profile is consistent with that of Hα and Hβ. In particular, the displaced blue peak is stronger than the red one, as required by the relativistic disk models.

Ultraviolet and far-infrared observations of Arp 102B have resulted in only weak detections. The *IRAS* coadded survey data reveal the source at 60 μm and 25 μm only, with fluxes of 0.29 and 0.28 Jy, respectively. The resulting peak in the νf_ν spectrum at 25 μm, while unusual for active galaxies, is very similar to the 25 μm component in 3C 390.3 (Miley *et al.* 1984). This is quite interesting in view of the fact that Arp 102B is similar to 3C 390.3 in its broad emission-line profiles. We obtained *IUE* exposures in both the short-wavelength and long-wavelength cameras on 1986 July 15, of duration 265 and 120 minutes, respectively. The continuum was detected only weakly in the 1600–3000 Å range at a level which is consistent with an extrapolation of the optical continuum. Table 1 summarizes the infrared and ultraviolet data, and Figure 7 shows the overall continuum, including near-infrared and optical points from Puschell *et al.* (1986) as well as the X-ray point of Biermann *et al.* (1981).

The only emission line detected in the ultraviolet is Lyα. Figure 8 shows the Lyα line, together with the Hβ profile shifted to the expected velocity. The Lyα peak agrees with the velocities of the narrow Hα and Hβ, but the width of Lyα is much less than that of the Balmer lines. There is no evidence for the blue and red peaks in the Lyα line. In fact, the red side of the Lyα line is consistent with the *IUE* resolution, so that approximately half of the flux may be coming from the narrow-line region. The total Lyα flux is 2.8×10^{-13} ergs cm^{-2} s^{-1}. A radiation hit very close to the spectrum at ~1240 Å was removed, but there may still be some contamination of the Lyα line at this wavelength. However, the line can be no wider than

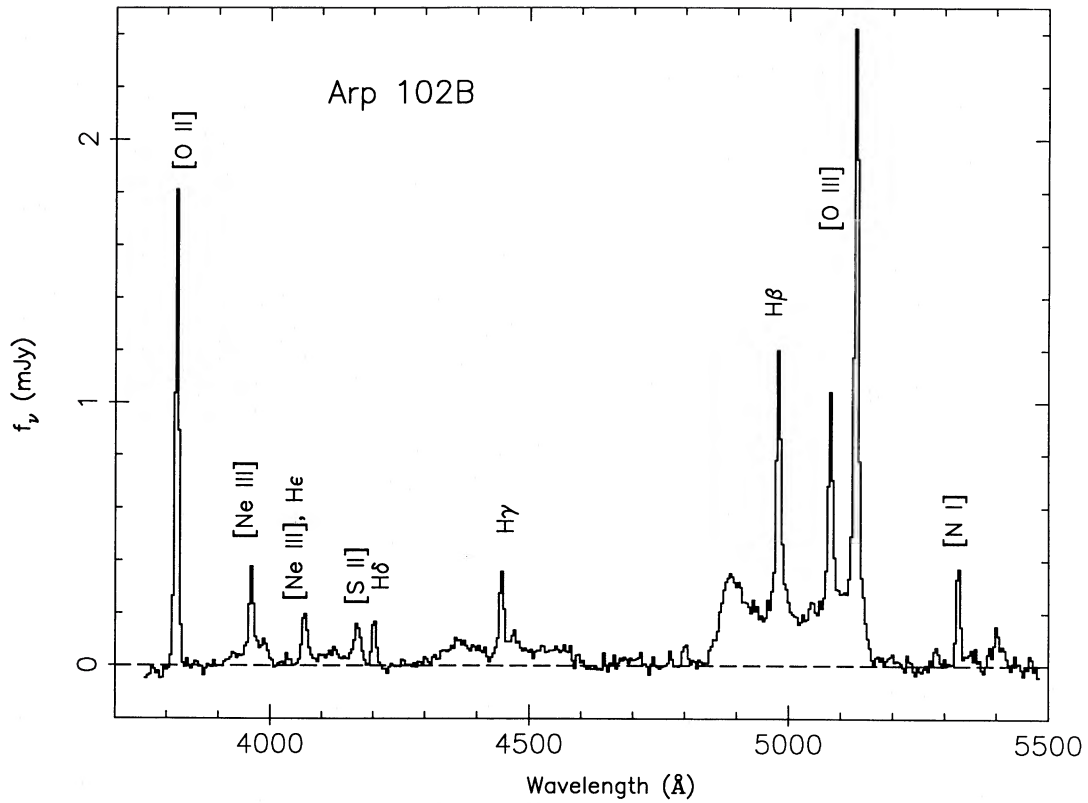

FIG. 5.—Emission-line spectrum of Arp 102B in the range 3760–5480 Å. The underlying stellar and nonstellar continua have been removed. Note the presence of broad Hβ and Hγ emission.

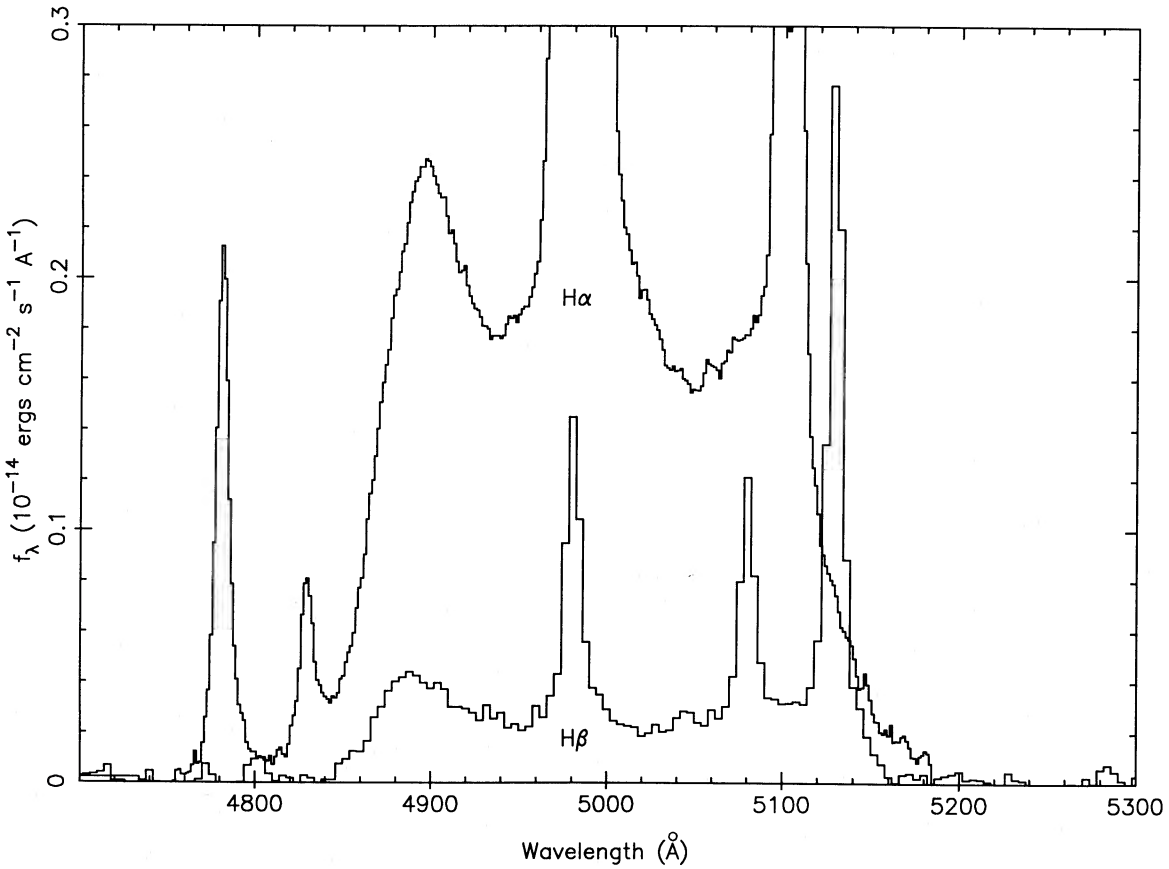

FIG. 6.—Hβ line of Arp 102B is superposed on the Hα line profile shifted to the expected velocity. The underlying stellar and nonstellar continua have been removed. The flux scale applies to Hβ. The scale of Hα has been adjusted to represent the true flux relative to Hβ.

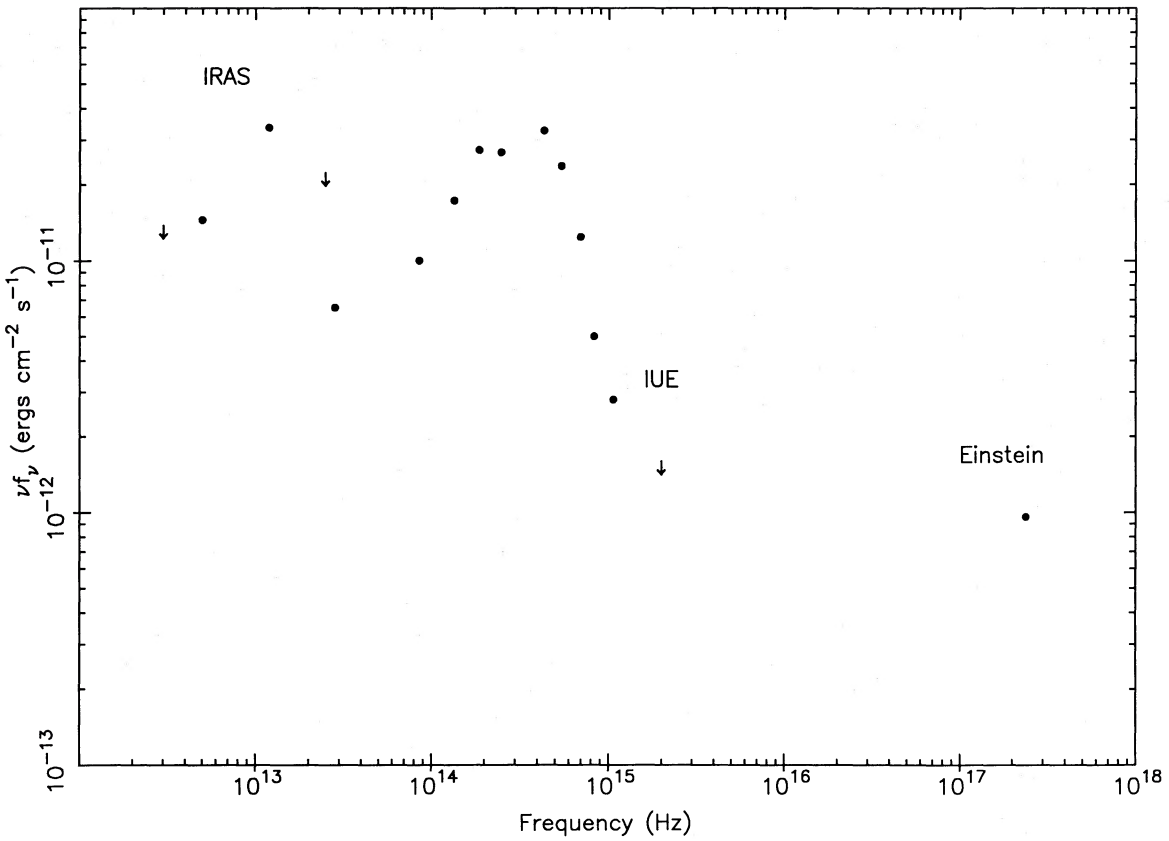

FIG. 7.—The continuum spectrum of Arp 102B including the near infrared and optical points from Puschell *et al.* (1986), and the X-ray point of Biermann *et al.* (1981). The remaining points are from Table 1.

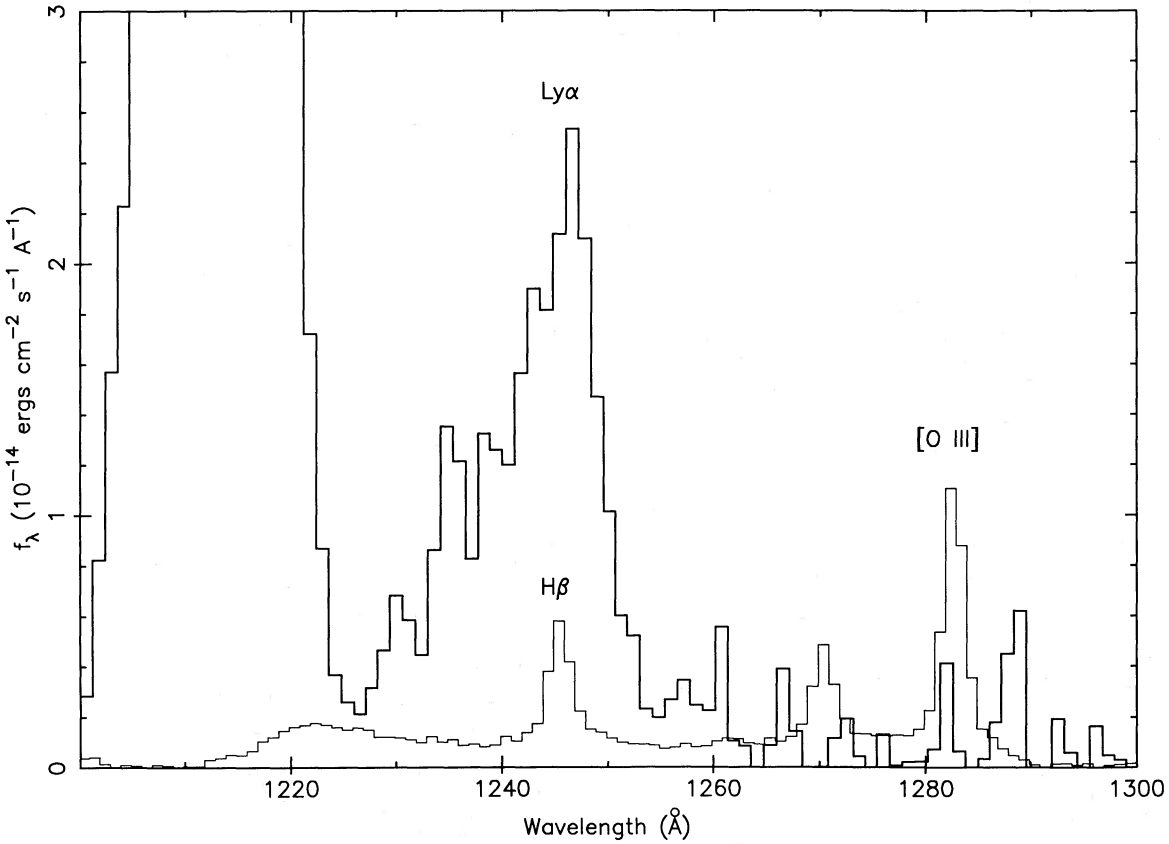

FIG. 8.—Lyα line of Arp 102B (*heavy line*) is superposed on the Hβ line profile (*thin line*) shifted to the expected velocity. The flux scale applies to Lyα. The scale of Hβ has been adjusted to represent the true flux relative to Lyα. Geocoronal Lyα dominates below 1225 Å.

that shown. If we attribute half the Lyα flux to the narrow-line region, then the ratio of narrow Lyα/Hβ is 12. The ratio of narrow Hα/Hβ is 4.3. These narrow-lines ratios are typical of moderately reddened ($E_{B-V} \simeq 0.3$) Seyfert galaxies (see Fig. 3 of Ferland and Osterbrock 1986). On the other hand, the virtual absence of broad displaced peaks in Lyα is probably due to large optical depths in the disk. For example, we may place an upper limit of ~ 1 on the ratio of Lyα/Hβ *at the wavelengths of the blue or red peaks.*

The overall continuum flux distribution of Arp 102B is not very different from that of other low-luminosity AGNs. The nonstellar UV continuum is difficult to detect in weak Seyfert nuclei, which are often first discovered by virtue of their X-ray emission. Although there is no evidence for a power-law or "big bump" spectrum in the ultraviolet, the X-ray detection indicates that adequate flux is likely present to account for the emission lines via photoionization. If we assume that the observed soft X-ray point lies on a ν^{-1} power law, then the flux between 1 and 1000 Rydbergs is 7×10^{-12} ergs cm^{-2} s^{-1}, as compared with 8×10^{-13} for the sum of the detected broad lines. Any UV bump, hard X-ray component, or soft X-ray absorption, would imply a further increase in this margin. Apparently, the disk need not intercept more than 10% of the flux of the ionizing source. An interesting comparison can be made with an X-ray selected elliptical Seyfert galaxy, NGC 6212 (Halpern and Filippenko 1986). This galaxy also has little or no nonstellar continuum, and, like 3C 390.3, a far-infrared spectrum which peaks at 25 μm (Neugebauer 1986). Perhaps elliptical Seyfert galaxies have a specific type of disk which is responsible for the far-infrared peaks at 25 μm as well as the broad emission lines.

We hypothesize that an ion-supported torus exists in the inner part of the disk. This theoretical construct was first proposed by Rees *et al.* (1982) to explain the jets in radio galaxies, which apparently have a very low accretion luminosity. In such a torus, the hot electrons in an equipartition magnetic field would radiate primarily synchrotron in the far-infrared, and the synchrotron self-absorption frequency would be $\sim 10^{13}$ Hz, or 30 μm (Rees *et al.* 1982). The extent of the torus in Arp 102B is probably bounded by the inner radius of the line-emitting region. Since the physics of the ion-supported torus is determined mainly by the quantity $\dot{m} = \dot{M}/\dot{M}_{\rm Edd}$, the similarity between Arp 102B and 3C 390.3 may indicate that they have roughly equal $\dot{m}$. The difference in absolute luminosity probably means that the mass of the black hole in Arp 102B is an order of magnitude smaller than that in 3C 390.3. Both the infrared spectrum and the line profile, considered together, could provide observational constraints on the accretion disk models. For example, if the accretion rate is very high (large $\dot{m}$), a radiation-supported torus may occupy the entire disk. If the accretion rate is very low (small $\dot{m}$), an ion-supported torus might occupy the entire disk. In either of these cases, the disk would be too hot to emit optical lines. Perhaps the broad lines in Arp 102B and 3C 390.3 occur only for an intermediate value of $\dot{m}$, for which an ion-supported torus is limited to the inner disk. The hot ion torus can then photoionize the outer, thin disk, causing it to emit lines.

V. CONCLUSIONS

We have calculated model emission-line profiles for a Keplerian disk which are correct to first order in M/r in the weak-field limit. When applied to the double-peaked Hα line profile of Arp 102B, the model can determine the inner and outer boundaries of the line-emitting region, ~ 250 and ~ 1000 in units of GM/c^2, and the inclination angle, $i = 33\overset{\circ}{.}5 \pm 5\overset{\circ}{.}5$. The gravitational energy liberated in a standard accretion disk at these radii is not much larger than the observed line emissivity, so an extra source of heating, possibly photoionization by radiation from the inner disk or central nonthermal source, may be required. We hypothesize the existence of ion-supported tori in radio galaxies such as Arp 102B and 3C 390.3 to account for the unusual far-infrared properties. Perhaps this type of disk is also conducive to the formation of optical emission lines in the outer regions.

Further study of this unusual AGN will require more sensitive detectors at ultraviolet and X-ray wavelengths in order to find spectroscopic evidence for a disk-like continuum. Continued monitoring of the emission-line profile, and observation of correlated continuum and line profile variations, could result in a direct measure of the absolute radius of the disk and therefore the mass of the black hole. The inner and outer boundaries of the Hα-emitting region have rotation periods of $0.4M_8$ and $3M_8$ yr, respectively, so that structural details of the disk could be revealed by just a few years of spectroscopic study.

We thank the staffs of the Goddard *IUE* Regional Data Analysis Facility, Palomar Observatory, and Lick Observatory for their expert assistance. This work was supported by NASA grant 5-823 to J. P. H., and by Cal Space grant CS-27-87 to A. V. F. In addition, observations at Lick Observatory were supported by NSF grant AST 86-14510 to the University of California. This article is contribution No. 353 of the Columbia Astrophysics Laboratory.

REFERENCES

Adler, R., Bazin, M., and Schiffer, M. 1975, *Introduction to General Relativity* (New York: McGraw-Hill), p. 218.
Begelman, M. C., Blandford, R. D., and Rees, M. J. 1984, *Rev. Mod Phys.*, **56**, 255.
Biermann, P., Kronberg, P. P., Preuss, E., Schilizzi, R. T., and Shaffer, D. B. 1981, *Ap. J. (Letters)*, **250**, L49.
Blandford, R. D., and McKee, C. F. 1982, *Ap. J.*, **255**, 419.
Collin-Souffrin, S. 1987, *Astr. Ap.*, **179**, 60.
Collin-Souffrin, S., Dumont, S., Heidemann, N., and Joly, M. 1980, *Astr. Ap.*, **83**, 190.
Czerny, B., and Elvis, M. 1987, *Ap. J.*, **321**, 305.
Ferland, G. J., and Osterbrock, D. E. 1986, *Ap. J.*, **300**, 658.
Filippenko, A. V. 1988, *Adv. Space Res.*, **8** (2), 5.
Filippenko, A. V., and Halpern, J. P. 1984, *Ap. J.*, **285**, 458.
Filippenko, A. V., and Sargent, W. L. W. 1988, *Ap. J.*, **324**, 134.
Gaskell, C. M. 1988, in *Proc. Georgia State University Conf. on Active Galactic Nuclei*, ed. H. R. Miller and P. J. Witta (New York: Springer-Verlag), p. 61.
Gerbal, D., and Pelat, D. 1981, *Astr. Ap.*, **95**, 18.
Halpern, J. P., and Chen, K. 1989, in *IAU Symposium 134, Active Galactic Nuclei*, ed. J. S. Miller and D. E. Osterbrock (Dordrecht: Reidel), in press.
Halpern, J. P., and Filippenko, A. V. 1986, *A.J.*, **91**, 1019.
———. 1988, *Nature*, **331**, 46.
Horne, K., and Marsh, T. R. 1986, *M.N.R.A.S.*, **218**, 761.
Kwan, J., and Krolik, J. H. 1981, *Ap. J.*, **250**, 478.
Luminet, J. P. 1979, *Astr. Ap.*, **75**, 228.
Malkan, M. A., and Sargent, W. L. W. 1982, *Ap. J.*, **254**, 22.
Mardaljevic, J., Raine, D. J., and Walsh, D. 1988, *Ap. Letters Comm.*, **26**, 357.
Mathews, W. G. 1982, *Ap. J.*, **258**, 425.
Miley, G., Neugebauer, G., Clegg, P. E., Harris, S., Rowan-Robinson, M., Soifer, B. T., and Young, E. 1984, *Ap. J. (Letters)*, **278**, L79.
Misner, C. W., Thorne, K. S., and Wheeler, J. A. 1973, *Gravitation* (San Francisco: Freeman), p. 674.
Neugebauer, G. 1986, private communication.
Oke, J. B. 1987, in *Superluminal Radio Sources*, ed. J. A. Zensus and T. J. Pearson (Cambridge: Cambridge University Press), p. 267.
Osterbrock, D. E., Koski, A. T., and Phillips, M. M. 1976, *Ap. J.*, **206**, 898.

Penston, M. V. 1988, private communication.
Perez, E., Penston, M. V., Tadhunter, C., Mediavilla, E., and Moles, M. 1988, *M.N.R.A.S.*, **230**, 353.
Puschell, J. J., Moore, R., Cohen, R. D., Owen, F. N., and Phillips, A. C. 1986, *A.J.*, **91**, 751.
Rees, M. J., Begelman, M. C., Blandford, R. D., and Phinney, E. S. 1982, *Nature*, **295**, 17.
Shakura, N. I., and Sunyaev, R. A. 1973, *Astr. Ap.*, **24**, 337.
Shields, G. A. 1978, *Nature*, **272**, 706.
Stauffer, J., Schild, R., and Keel, W. 1983, *Ap. J.*, **270**, 465.
Sun, W.-H., and Malkan, M. A. 1988, in *Supermassive Black Holes*, ed. M. Kafatos (Cambridge: Cambridge University Press), p. 273.
Tylenda, R. 1981, *Acta Astr.*, **31**, 127.
van Groningen, E. 1983, *Astr. Ap.*, **126**, 363.
Wandel, A., and Mushotzky, R. F. 1986, *Ap. J. (Letters)*, **306**, L61.
Williams, R. 1980, *Ap. J.*, **235**, 939.

KAIYOU CHEN and JULES P. HALPERN: Columbia Astrophysics Laboratory, Columbia University, 538 West 120th Street, New York, NY 10027

ALEXEI V. FILIPPENKO: Astronomy Department, University of California, Berkeley, CA 94720